JOURNAL OF MATERIALS SCIENCE 29 (1994) 3102–3106

# The processing and electrical properties of plasma-sprayed yttria–zirconia

C. L. CURTIS, D. T. GAWNE
*Department of Materials Technology, Brunel The University of West London, Uxbridge, Middlesex, UK*

M. PRIESTNALL
*Cookson Technology Centre, Oxford, UK*

The electrical conductivity of yttria-stabilized zirconia produced by plasma spraying was investigated with special reference to fuel-cell applications. The results show that the grain-boundary conductivity of plasma-sprayed yttria–zirconia increases with decreasing precursor-particle size. Small particles are shown to melt more completely in the plasma, and their improved flow on the deposit reduces intersplat porosity and the barriers to oxygen-ion transport. The grain-interior conductivity also increases with decreasing precursor-particle size, owing to the diminishing presence of the monoclinic phase in the deposit. Yttria is homogenized in the small particles during plasma spraying, which suppresses the monoclinic transformation on cooling.

## 1. Introduction

Fuel cells convert the chemical energy of a reaction directly into electrical energy, providing a clean and efficient source of energy conversion. Solid-oxide fuel cells are generally recognized as having the greatest potential for large-scale commercial applications [1], and zirconia-based ceramics are particularly attractive candidate materials. Besides showing good mechanical stability, the ionic conductivity of zirconia can be markedly increased at elevated temperatures by forming a solid solution in which some of the tetravalent zirconium ions are replaced by trivalent yttrium ions, since the necessary charge compensation generates oxygen-ion vacancies which enable oxygen-ion migration [2, 3].

Solid-oxide electrolytes have been previously prepared by sintering, tape casting, chemical vapour deposition, physical vapour deposition and slurry coating [4, 5]. This paper concerns plasma spraying, which has potential advantages as a production process for solid-oxide electrolytes in terms of material design and manufacturing flexibility. The purpose of the present work is to investigate the influence of the precursor-particle size on the electrical conductivity and structure of 8 wt % yttria–zirconia.

## 2. Materials and techniques

The powder samples used in this investigation were prepared from Metco 204 NS (Metco Ltd, Chobham, UK), an 8 wt % yttria-stabilized zirconia. The as-received powder was sieved into five size intervals and each fraction was designated by its average size: 20–38 μm (designated as 30), 38–52 μm (45), 52–75 μm (65), 75–90 μm (80) and 90–110 μm (100).

The six classes of powder were deposited on 304-grade stainless steel (18 wt % chromium, 10 wt % nickel, 0.05 wt % carbon) using a Metco MN plasma-spray system. Spraying was carried out in air with a stand-off distance of 100 mm to give deposits approximately 0.5 mm in thickness. The microstructures of the fractured cross-sections of the deposits were observed using scanning electron microscopy (SEM) and light microscopy. In order to gain an insight into the mechanisms of the formation of the deposits, wipe tests were undertaken in which glass slides were plasma sprayed using an extremely fast gun traverse speed to give the deposition of isolated splats. These slides were examined using a scanning electron microscope enabling the extent of flow of individual particles on impact with the substrate to be observed. X-ray diffraction (XRD) was used to determine any changes in structure occurring during plasma spraying with respect to the initial feed powder. The bulk densities of the deposits were determined at 20 °C by the mercury-upthrust technique using a Doulton Densometer.

## 3. Results and discussion

### 3.1. Conductivity

The electrical conductivities of the samples were measured by the complex-impedance method using a Schlumberger 1260 impedance-gain phase analyser over the frequency range 100 mHz to 10 MHz. The experimental apparatus was interfaced with a microcomputer in order to process the data. Gold contacts, 5 mm by 5 mm, were sputtered onto both sides of the samples and connected to 5 mm by 5 mm platinum



0022–2461 

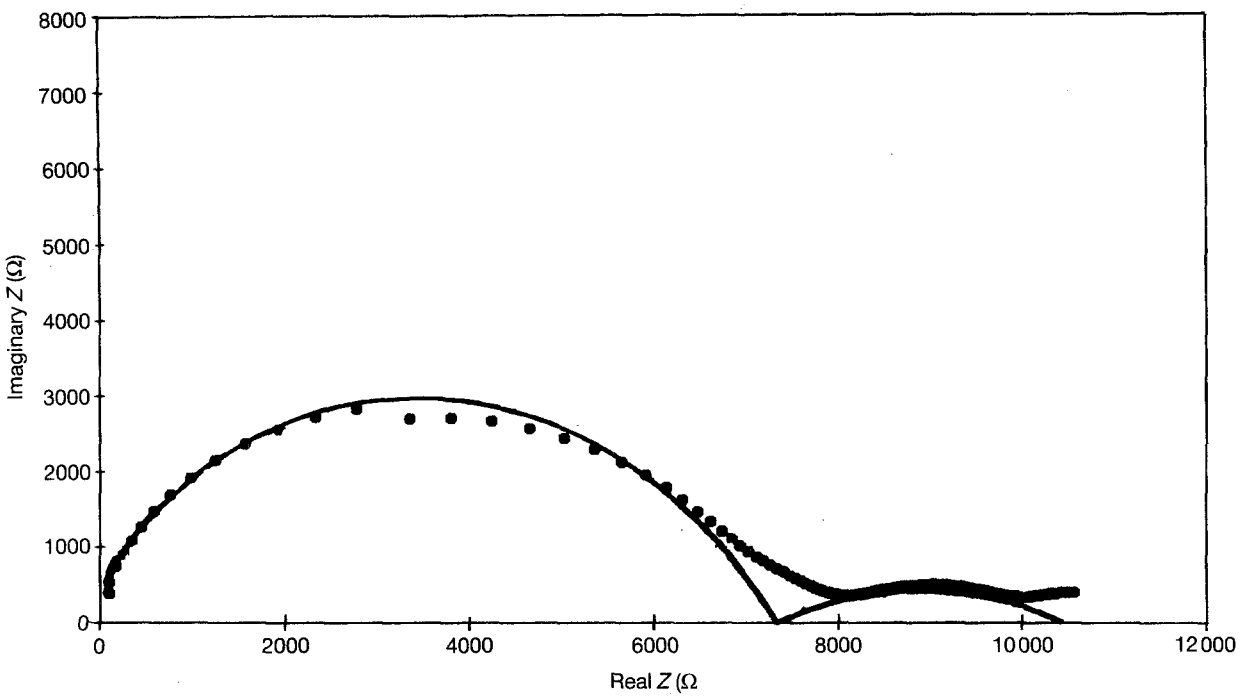


*Figure 1* A Nyquist diagram for the YSZ deposit plasma sprayed with the 30-particle-size-range powder.

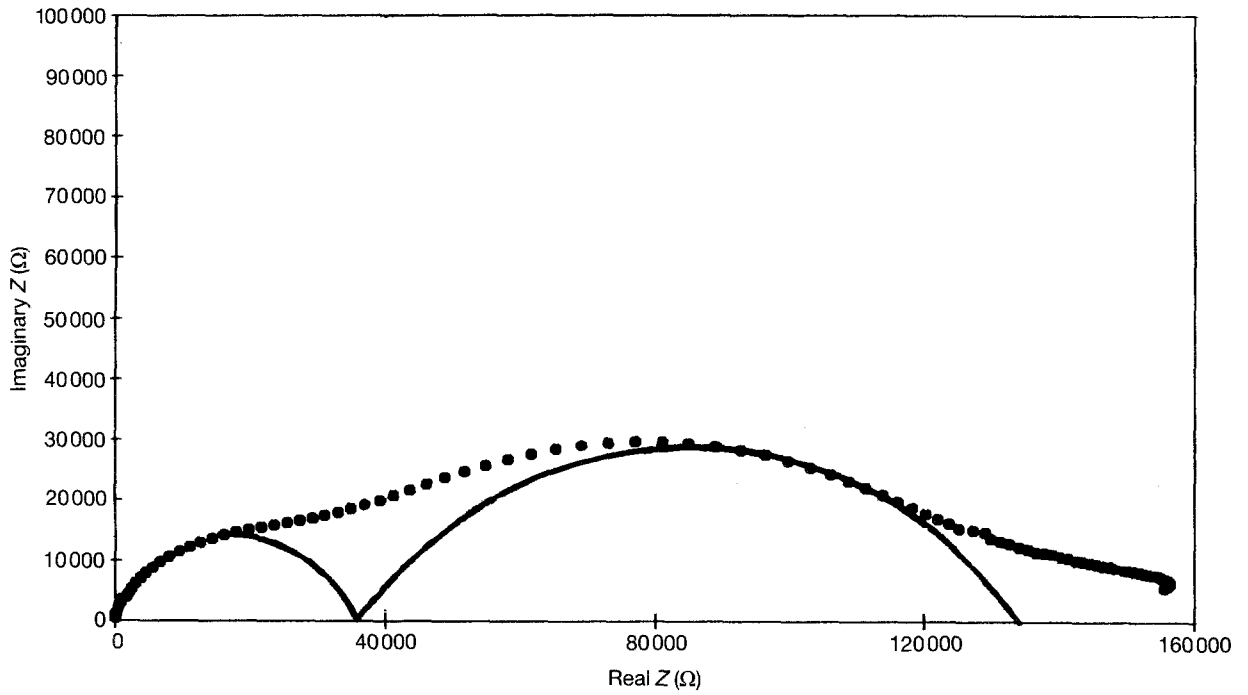


*Figure 2* A Nyquist diagram for the YSZ deposit plasma sprayed with the 100-particle-size-range powder.

gauze by silver paint to enable measurements to be made at 380 °C.

The conductivity data are expressed as Nyquist diagrams in which the imaginary impedance is plotted against the real impedance (Figs 1 and 2). The locus of the points generally describe two semicircles: the semicircle at the higher frequency on the left relates to the grain-interior resistance and the one at the lower frequency relates to the grain-boundary resistance. Figs 1 and 2 reveal significant changes in the impedance characteristics between samples plasma sprayed with different precursor-particle sizes. Table I shows

TABLE I Grain-interior and grain-boundary conductivities

| Sample | Particle Size (μm) | Conductivities $(\mu\Omega\,cm)^{-1}$ | |
|---|---|---|---|
| | | Grain interior | Grain boundary |
| 30 | 20–38 | 63.4 | 141 |
| 45 | 38–52 | 30.3 | 27.7 |
| 65 | 52–75 | 20.7 | 7.38 |
| 80 | 75–90 | 10.9 | 3.79 |
| 100 | 90–110 | 9.44 | 3.45 |
| 204NS | 20–110 | 23.7 | 25.8 |

the impedance data obtained for the samples under investigation.

## 3.2. Formation of deposits

Fig. 3 shows that the porosity of the plasma-sprayed coatings decreases with decreasing precursor-particle size. The SEM analysis showed that the deposits exhibited a lamellar structure parallel to the deposit surface with fine columnar grains through the thickness of each lamella (Figs 4 and 5).

The microstructure of the coatings may be understood in relation to the physical processes in plasma spraying. The precursor powder is injected into the plasma, where it is melted in flight to form a molten droplet. On impact with the substrate, the droplet spreads out laterally over the surface and rapidly solidifies to form a disc-shaped lamella or splat (Fig. 6). The deposit is built up from numerous overlapping splats as the plasma gun traverses over the substrate. Figs 7 and 8 show the results of wipe tests in which isolated splats are produced: a splat is generally thicker at the centre, since solidification will occur first at the periphery which then prevents further spread of material. The molten splat cools rapidly by heat conduction to the substrate and air so that the greatest heat-flow rate will be perpendicular to its surface. Crystallization is initiated by heterogeneous nucleation at the underlying splat surfaces, and subsequent growth of the crystals into the molten splat along the principal heat-flow direction results in the formation of columnar grains through the splat thickness. The

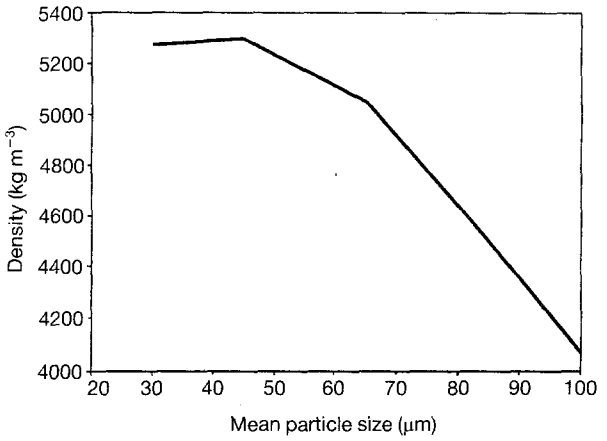


*Figure 3* The influence of the precursor-particle size on the density of the plasma-sprayed YSZ.

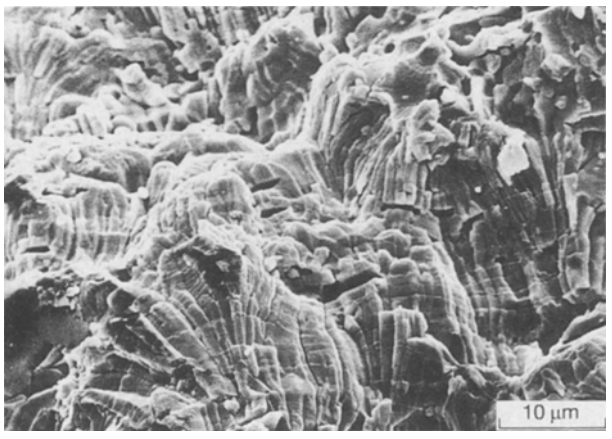


*Figure 4* A scanning electron micrograph of the YSZ deposits plasma sprayed with the 30-particle-size-range powder.


*Figure 5* A scanning electron micrograph of the YSZ deposits plasma sprayed with the 100-particle-size-range powder.

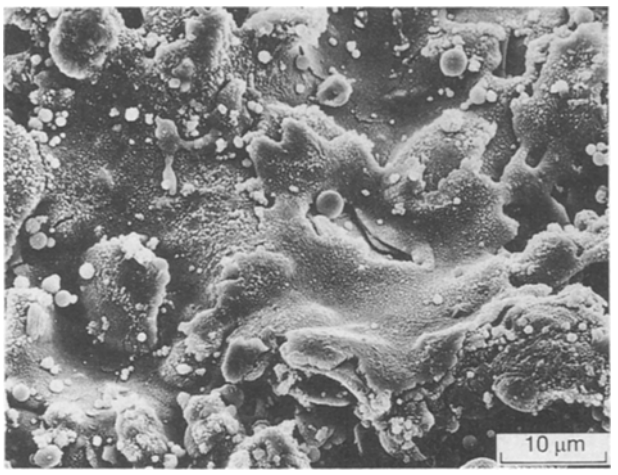


*Figure 6* A scanning electron micrograph of the top surface of a YSZ-plasma-sprayed deposit.

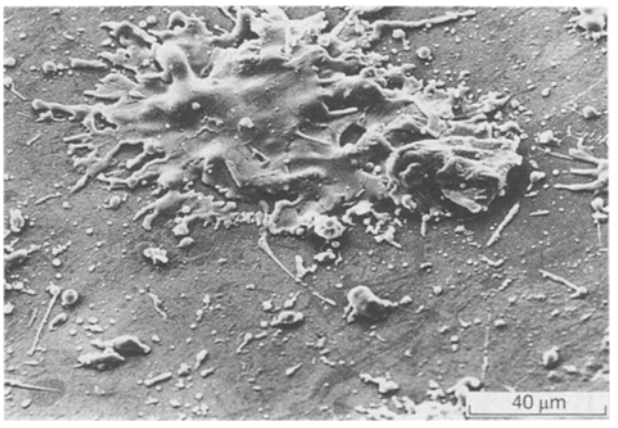


*Figure 7* A scanning electron micrograph of individual splats produced in a wipe test using the 30-particle-size-range powder.

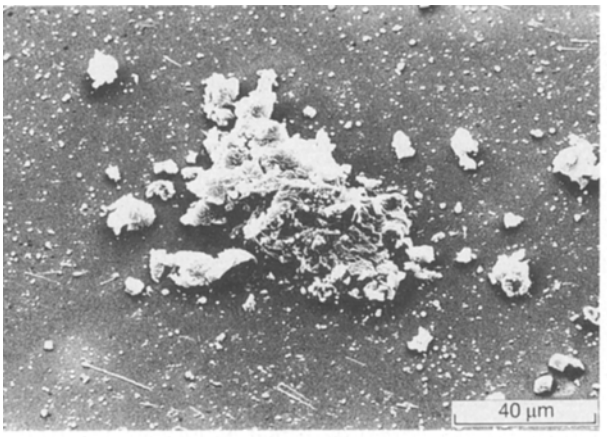


*Figure 8* A scanning electron micrograph of individual splats produced in a wipe test using the 80-particle-size-range powder.

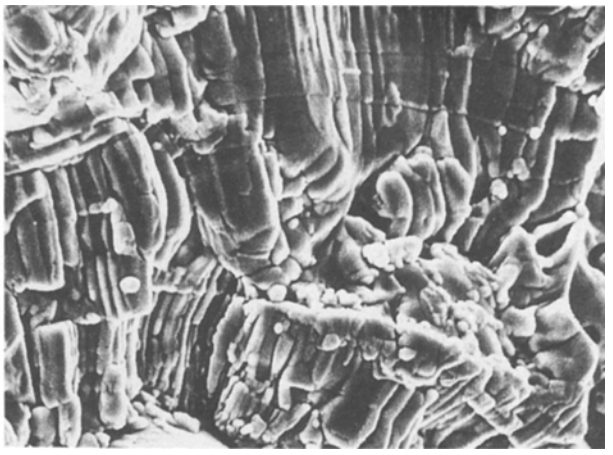

*Figure 10* Scanning electron microscopy of the YSZ deposit plasma sprayed with the 30-particle-size-range powder.

rapid cooling rate and high degree of undercooling generates a high nucleation rate which is responsible for the extremely fine columnar grain structure observed in Figs 4 and 5.

## 3.3. Structure dependence of conductivity

### *3.3.1. Macrostructure*

The porosity caused by the inadequate flow of splats, particularly from coarse precursor powders, will be located at the boundaries between neighbouring splats. The presence of pores at the splat boundaries will present a major obstacle to the transport of oxygen ions through the deposit; this is considered to be the source of the increase in the grain-boundary resistivity with increasing precursor-particle size that is shown in Fig. 9.

The porosity is virtually the same for samples 30 and 45 (Fig. 3) whereas the conductivity of sample 30 is markedly higher (Table I). Closer examination of the deposits revealed that there was much more columnar grain growth across the splat boundaries from one splat to its neighbour in sample 30, produced from the finest precursor powder, than in the other deposits, as is evident in Figs 4, 5 and 10.

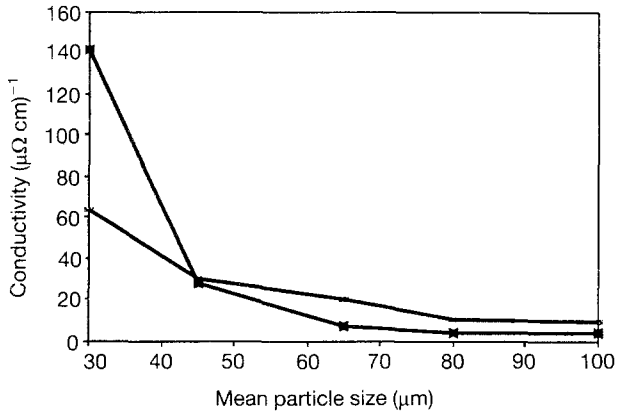


*Figure 9* The relationship between ( − ) the grain-boundary conductivity, (*) the grain-interior conductivity and precursor-particle size.

Intersplat grain growth is indicative of the close contact and sound bonding between splats due to the extensive flow of the small precursor particles during the formation of sample 30. Although the inferior misfit across the splat boundaries in sample 45 is not detectable from density measurements, it is an effective barrier on the microscopic scale in which ion transport takes place. It is also evident that the presence of an extremely fine columnar grain structure in sample 30 does not significantly impair its electrical conductivity.

These results indicate that the dominant contribution to grain-boundary impedance is the blocking effect of the splat boundaries rather than that of the columnar-grain boundaries.

### *3.3.2. Microstructure*

In principle, the presence of 8 wt % yttria should be sufficient to stabilize the high-temperature tetragonal and cubic zirconia phases against transformation on cooling to the monoclinic structure [6]. However, the X-ray diffractometer profile from the precursor powder shown in Fig. 11a exhibited (111) and ($11\bar{1}$) monoclinic peaks on either side of a large (111) tetragonal/cubic peak as shown in Fig. 11a. The monoclinic phase tends to form at low dopant levels and in this case its presence is attributed to the lack of stabilization of zirconia in regions of low yttria content created during the powder manufacturing process. Fig. 11b and 11c show that the monoclinic phase is absent from the deposit prepared from the fine precursor powder (sample 30) but it is still present in the deposit prepared from the coarse powder (sample 100). These results indicate that the complete melting of the particles from sample 30 in the plasma homogenizes the yttria throughout the alloy thereby suppressing the formation of the monoclinic phase on solidification. The coarser particles from sample 100 do not completely melt owing to the larger thermal diffusion distances into their cores and so some low-yttria pockets remain with the accompanying monoclinic phase in the deposit.

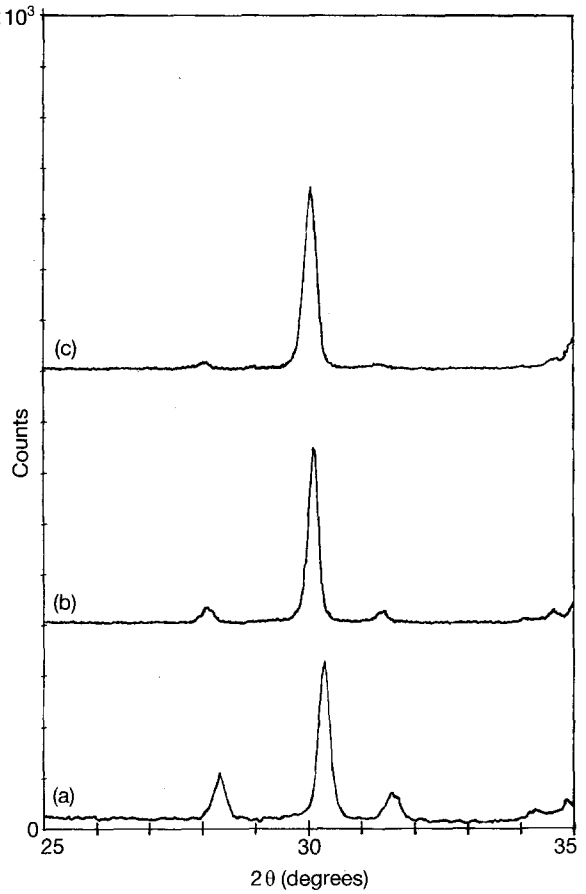


*Figure 11* X-ray-diffractometer profiles for the following precursor-powder sizes: (a) as-received, (b) 90–110 μm, and (c) 20–38 μm.

It has been established [7] that the ionic conductivities of both the cubic and tetragonal phases are significantly greater than those of the monoclinic phase. The increasing presence of the monoclinic phase as the precursor-particle size increases is therefore considered to be the basis of the relationship between the grain-interior-impedance, $\sigma_i$ and the powder size found in Fig. 9.

## 4. Conclusion

1. The grain-boundary conductivity of plasma-sprayed yttria-stabilized zirconia is dominated by the splat boundaries, with the columnar grain boundaries having no noticeable effect.

2. The grain-boundary conductivity of plasma-sprayed yttria-stabilized zirconia increases with decreasing precursor-particle size. Small particles are shown to melt more completely in the plasma, and their improved flow on impact with the substrate reduces intersplat porosity and the barriers to oxygen-ion transport.

3. The grain interior conductivity also increases with decreasing precursor-particle size owing to the diminishing presence of the monoclinic phase in the deposits. Yttria is homogenized in the small particles during plasma spraying, which suppresses the transformation on cooling to the monoclinic structure.

## Acknowledgements

The authors wish to thank the Science and Engineering Research Council and the Cookson Group plc for permission to publish this paper.

## References

1. E. IVERSTIFFEE, W. WERSING, M. SCHIESS and H. GREINER, *Ber. der Bunsen Gesellshaft fur Phys. Chemie*, **9** (1990) 978.
2. K. R. WILLIAMS, "An introduction to fuel cells", (Elsevier, Amsterdam, 1966).
3. K. KIUKKOLA and C. WAGNER, *J. Electrochem. Soc.* **104** (1957) 379.
4. A. O. ISENBERG, Procedures of the symposium on Electrode Materials And Processes For Energy Conversion And Storage (Electrochemical Society, 1977) 572.
5. M. SCAGLIOTTI, F. PARMIGIANI, G. CHIODELLI, A. MAGISTRIS, G. SAMOGGIA and G. LANZI, *Solid State Ionics*, **28–30** (1988) 1766.
6. A. H. HEUER and L. W. HOBBS (editors) "Science and technology of zirconia I", Advances in Ceramics, Vol. 3 (American Ceramic Society, Westerville, Ohio, 1981).
7. N. BONANOS, R. K. SLOTWINSKI, B. C. H. STEELE and E. P. BUTLER, *J. Mater. Sci.* **19** (1984) 785.

*Received 16 September*
*and accepted 8 October 1993*